JOURNAL OF GEOPHYSICAL RESEARCH, VOL. 114, D13103, doi:10.1029/2008JD011103, 2009

Diurnal variation of precipitation over southeastern China: Spatial distribution and its seasonality

Guixing Chen,[1] Weiming Sha,[1] and Toshiki Iwasaki[1]

Received 4 September 2008; revised 23 March 2009; accepted 4 May 2009; published 10 July 2009.

[1] Using the satellite data, spatial patterns of precipitation diurnal cycles and their seasonality were examined with emphasis on southeastern China (SEC). Results show that spatial distributions of diurnal cycles over SEC have a robust large-scale seasonality in which the regional differences are evidently embedded. Rainfall diurnal variability is weak in spring but it becomes more pronounced from presummer. Both the mean rain rates and amplitudes of diurnal cycles experience remarkable amplification during presummer. The widespread and strong morning rainfall dominates the SEC area, especially inland valleys and plains, and offshore areas. The morning peak rainfall over western SEC is largely contributed by the increasing rain frequency and diurnally varying intense rain rates. Even over eastern SEC, morning rainfall still has a comparable magnitude to afternoon rainfall. In contrast, spatial distributions of diurnal cycles in midsummer are dependent primarily on topography. The morning (afternoon) rainfall is mainly located over valleys, basins, and oceans (plateaus and mountains). The afternoon peak rainfall becomes a notable feature over southern China. The signature of widespread morning rainfall decays during midsummer and remains apparent only in central eastern China, which is likely related to the north shift of summer rainband.

Citation: Chen, G., W. Sha, and T. Iwasaki (2009), Diurnal variation of precipitation over southeastern China: Spatial distribution and its seasonality, *J. Geophys. Res.*, *114*, D13103, doi:10.1029/2008JD011103.

1. Introduction

[2] In East Asia (Figure 1), precipitation and cloudiness not only show a distinct seasonal transition [e.g., *Tao and Chen*, 1987; *Ding*, 1992]; they also exhibit pronounced diurnal variability [e.g., *Nitta and Sekine*, 1994; *Ohsawa et al.*, 2001]. Along with the monsoon progress, the East Asian rainband marches northward in a stepwise manner. It is established over South China Sea and southern China in mid-May, and subsequently extends to Yangtze River Valley and southwestern Japan in mid-June. It finally passes to northern China, Korea, and Japan in midsummer. On both seasonal and diurnal timescales, the huge amount of latent heat released by frequent heavy rains is considered an important driving force of the Asian summer monsoon circulation [*Luo and Yanai*, 1984; *Johnson et al.*, 1993].

[3] The spatial diversity of diurnal variation in precipitation over East Asia has been examined extensively using satellite, radar and rain gauge data. During the warm season, diurnal variation is evident with a pronounced topographic effect. The diurnal variation of convective activities is great over the continents, large islands, and their adjacent seas, although it is less pronounced over the oceans [*Takeda and Iwasaki*, 1987; *Nitta and Sekine*, 1994]. Late night to early morning convective activities in the tropical Asia are found to occur often in the windward mountains, basins and valleys, and coastal regions [*Ohsawa et al.*, 2001]. *Hirose and Nakamura* [2005] examined the diurnal-scale features of precipitation systems according to their scale sizes. They found that small systems occurred frequently in the early afternoon over landmasses, although large ones developed in the evening over near-flat areas. As described above, diurnal variation differs regionally because of the modulation of low-level convergence by land/sea and mountain/valley breezes in addition to mesoscale features.

[4] Another unique impact of topography is the downward propagation of rainfall episodes in leeward areas of high terrain. It explains the morning maximum of precipitation frequency immediately east of the Rocky Mountains [*Wallace*, 1975; *Carbone et al.*, 2002]. To the east leeward of the Tibetan Plateau, diurnal variation of cloudiness undergoes a similar phase delay [*Asai et al.*, 1998; *Wang et al.*, 2004]. Using hourly rain gauge data, *Yu et al.* [2007a] confirmed that diurnally varying precipitation in the Sichuan Basin peaked around midnight and exhibited a phase delay further east. Different from North America, the phase shift phenomenon over East Asia is strongest in presummer and declines clearly in midsummer, implying a dramatic seasonal change [*Asai et al.*, 1998; *Wang et al.*, 2004].

[5] The spatial distribution of diurnal variability tends to be inhomogeneous because of various physical processes. China is a key region with high spatiotemporal variation of diurnal cycle; it should be resolved in detail [*Hirose and Nakamura*, 2005]. In particular, southeastern China (SEC),

[1]Department of Geophysics, Graduate School of Science, Tohoku University, Sendai, Japan.

0148-0227/09/2008JD011103$09.00

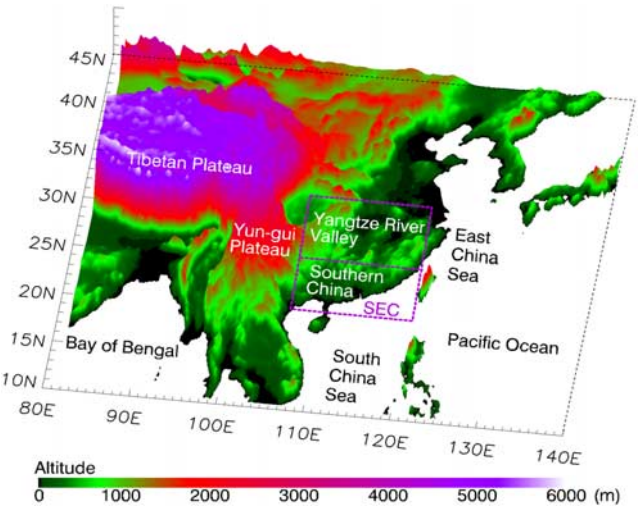

Figure 1. Topography of East Asia. The rectangle (105–120°E, 20–32°N) encloses southeastern China (SEC) including southern China (20–25°N) and Yangtze River Valley (25–32°N). The Yun-gui Plateau is located west of the SEC.

located to east of the Tibetan Plateau and north of South China Sea (Figure 1), is probably affected by complex terrain, land-sea contrast and monsoon flow. Earlier studies have addressed this topic from a wide perspective, using GMS data as a rainfall proxy [e.g., *Nitta and Sekine*, 1994] or using rain gauge data available only on land [*Yu et al.*, 2007a]. To date, studies of diurnal variation during summer transition have been few. Fortunately, the studies described above have provided a wealth of information, which aids our effort to give a detailed picture of diurnally varying phenomena over SEC.

[6] The present study emphasizes the SEC area, where the East Asian rainband originates and begins its remarked seasonal march. It is intended to discern representative patterns of diurnal cycles in precipitation. Section 2 provides a description of the data and methods used for this study. The seasonal variation of rainfall budget over the SEC area is examined in section 3. Section 4 is devoted to describing the spatial distribution of rainfall diurnal cycles and their seasonal changes. Section 5 presents an investigation of the regional contrasts of rainfall diurnal cycles over the SEC area. Finally, a summary and discussion are presented.

2. Data and Methods

[7] To describe the remarked summer transition over SEC, we group the data into those of spring (March–April), presummer (May–June), and midsummer (July–August). In general, the summer monsoon is established over South China Sea in middle to late May. Accordingly, the East Asian rainband remains over southern China from May to early June; afterward it shifts to Yangtze River Valley in mid-June [*Tao and Chen*, 1987; *Ding*, 1992]. Consequently, presummer, as defined herein, is a crucial season: it includes the early stage of summer monsoon and the first rainy season over SEC.

2.1. Tropical Rainfall Measuring Mission Data

[8] Since the end of 1997, the Tropical Rainfall Measuring Mission (TRMM) satellite, equipped with the TRMM Microwave Imager (TMI) and Precipitation Radar (PR), has offered a unique opportunity for detecting the spatial variation of precipitation on both diurnal and seasonal timescales. These archived data of a long period have been used for reliable estimation of rain properties throughout the global tropics (±36° latitude) [e.g., *Nesbitt and Zipser*, 2003; *Nesbitt et al.*, 2006]. The data have fostered some insights into underlying processes of diurnal variation [*Nesbitt and Zipser*, 2003; *Yang and Smith*, 2006]. Such fine-scale data are particularly helpful for resolving diurnal variation over the complex terrain such as that of East Asia (Figure 1).

[9] This study uses the TRMM-TMI product (3G68) to seek the major patterns of diurnal variation over SEC. With a scanning swath of 760-km width from a sun-asynchronous orbit, it provides 0.5° gridded values of the total pixels, rainy pixels, mean rain rate, and the percentage of convective rain. For a given grid over SEC, the 2-month sampling for 1-h intervals is 3–7 with a mean of 5. The time lag of diurnal cycles in sampling after 1 year is about 3 h. The 9-year TRMM archive can yield even sampled hourly data and thereby greatly improve the temporal sampling. We calculate the hourly variables for each local hour in spring, presummer and midsummer. Then these hourly data are processed with a ±2-h running mean to smooth the temporal variation. For any given hour, any grid over SEC can yield a signal available at 25 days among two months. Hourly data of the rain probability can be estimated with the rainy pixels divided by the total pixels.

[10] As described above, the temporal sampling of TRMM-TMI data is highly coarse at a specific location. For locally continuous observations, TRMM-3B42 rainfall (3 hourly, 0.25°) is used for this study. This product is derived by using an optimal combination of the microwave precipitation estimates from TRMM and other microwave measurements to adjust the infrared precipitation estimates from geostationary satellite. It is scaled to match the monthly rain gauge measurements. *Zhou et al.* [2008] recently revealed that TRMM-3B42 estimate was somewhat reliable for measuring the spatial patterns of precipitation over contiguous China.

2.2. Cluster Analysis of TRMM Data

[11] The following processes are performed to seek representative patterns of diurnal cycles and their spatial distributions. First, we obtain TRMM-TMI hourly variables as described in section 2.1; then we apply Fourier analysis to the hourly rain rate at each grid. The first three harmonic components are retained to represent the diurnal cycle of variation. Then fuzzy c mean cluster analysis is used to search for typical patterns. A full description of details of this method is presented in an earlier study [*Fujibe*, 1999]. This method presents some advantages for obtaining a few clusters from among voluminous data; it differs from other cluster analyses in that it enables partial membership of stations to clusters. The major patterns of rainfall diurnal cycles are constructed using the memberships and hourly series from all grids. Spatial distributions of these major patterns are shown by the maximum memberships at grids.

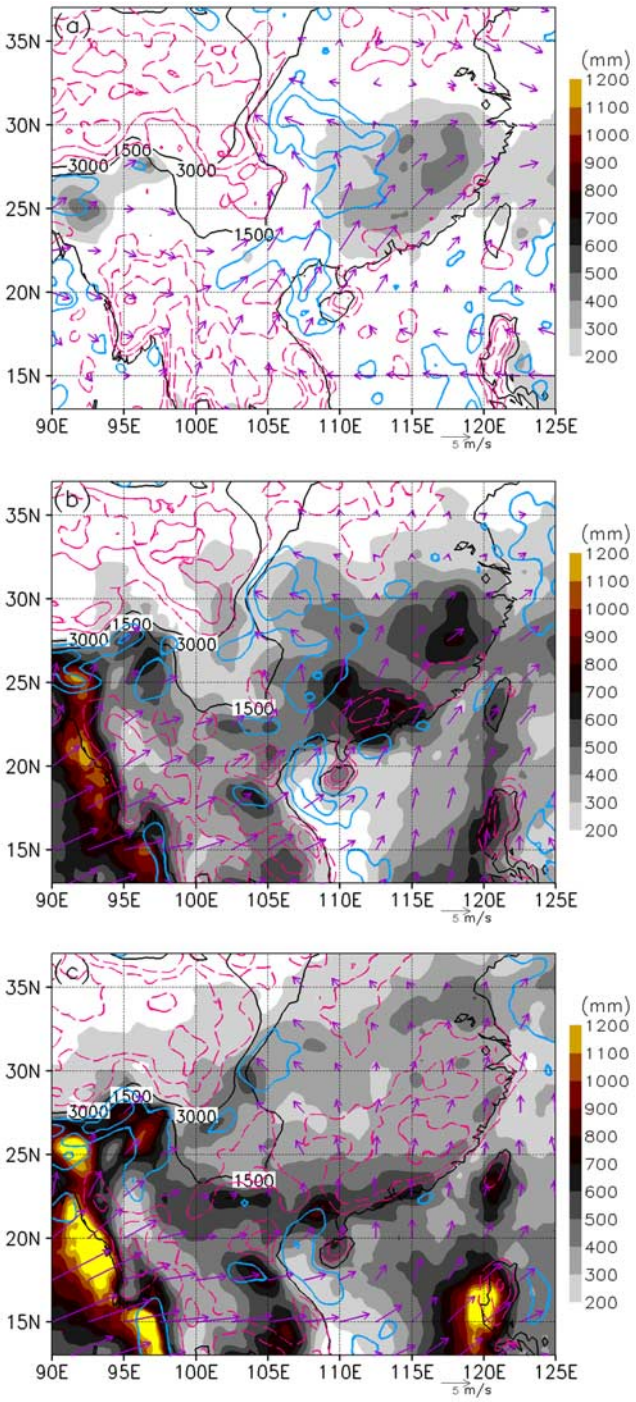

Figure 2. Mean seasonal rainfall budget in TRMM-3B42 estimate (1998–2006) for (a) spring, (b) presummer, and (c) midsummer. Rainfall accumulation greater than 200 mm is shaded. Rainfall difference between 0000–1200 and 1200–2400 LT expressed as a percentage of the mean daily rainfall is shown in contour; solid (dashed) contours stand for positive (negative) values with an interval of 20%. Vector shows the 850-hPa wind in NCEP reanalysis data (1998–2006). Elevations of 1500 and 3000 m are marked.

[12] The standard deviations of year-to-year variation of the extracted diurnal cycles show the robustness of cluster analysis. They are much smaller than either the mean value or the amplitude of diurnal oscillation (see Figures 3–5). To verify the results from the TRMM-TMI data, cluster analyses are also applied to the TRMM-PR rainfall. The results (not shown) resemble those shown in Figures 3–5, but they are dispersed slightly because the samples are fewer: the latter uses a narrower scanning swath. Analysis of the TRMM-3B42 data on a diurnal scale is also undertaken. The major patterns are shown consistently, but not in a clear manner, as Figures 3–5.

3. Seasonal Change of Rainfall Budget Over SEC

[13] The mean seasonal rainfall budget from spring to midsummer is examined in Figure 2. Rainfall amount averaged over the SEC area is 213, 468 and 412 mm in spring, presummer and midsummer, respectively. Rainfall accumulation (1093 mm) from March to August accounts for 75% of the annual rainfall budget (1463 mm); it is consistent to the results by rain gauge observations [*Li et al.*, 2008]. Figure 2a shows that the spring rainfall is relatively weak and mainly located over SEC and East China Sea, with rainfall maximum to the west of the Wu-yi-shan mountain range along east coast.

[14] During presummer, precipitation undergoes a remarkable increase over Bay of Bengal and South China Sea where the summer monsoon commences (Figure 2b). The strong rainfall is also observed over the SEC area; several centers of maximum rainfall appear along coastal inland and over western region of SEC. The seasonal rainfall over SEC reaches its maximum during May–June, which is known as presummer rainy season for southern China and Meiyu period for Yangtze River Valley [*Tao and Chen*, 1987; *Ding*, 1992]. During midsummer, the strong rainfall is still visible along southern China coast, while the rainfall over other regions of SEC decays slightly (Figure 2c). A rainfall zone stretching from southwest (Sicuan Basin) to northeast is readily observed in central eastern China (to the north of SEC). It is probably related to the northward shift of the summer rainband since mid-July [*Ding*, 1992].

[15] Figure 2 also sketches the rainfall budget difference between morning hours (0000–1200 LT) and afternoon hours (1200–2400 LT) precipitation expressed as a percentage of the mean daily precipitation. It indicates the relative amplitude of diurnal rainfall cycle. Over the Tibetan Plateau and tropical regions, rainfall amount during afternoon hours exceeds that during morning hours by 40% or more. Seasonal change of the subdaily difference in rainfall is readily observed over the SEC area. During spring and presummer, in excess of 20% more precipitation falls during morning hours than during afternoon hours on the east flank of plateaus and over western SEC. Even over eastern SEC, rainfall amount of morning hours has a comparable magnitude to that of afternoon hours. In presummer, afternoon hour rainfall becomes apparent along southern China coast, while morning hour rainfall appears offshore. In midsummer, afternoon hour rainfall dominates the inland regions of SEC, especially southern China. Along the rainband to

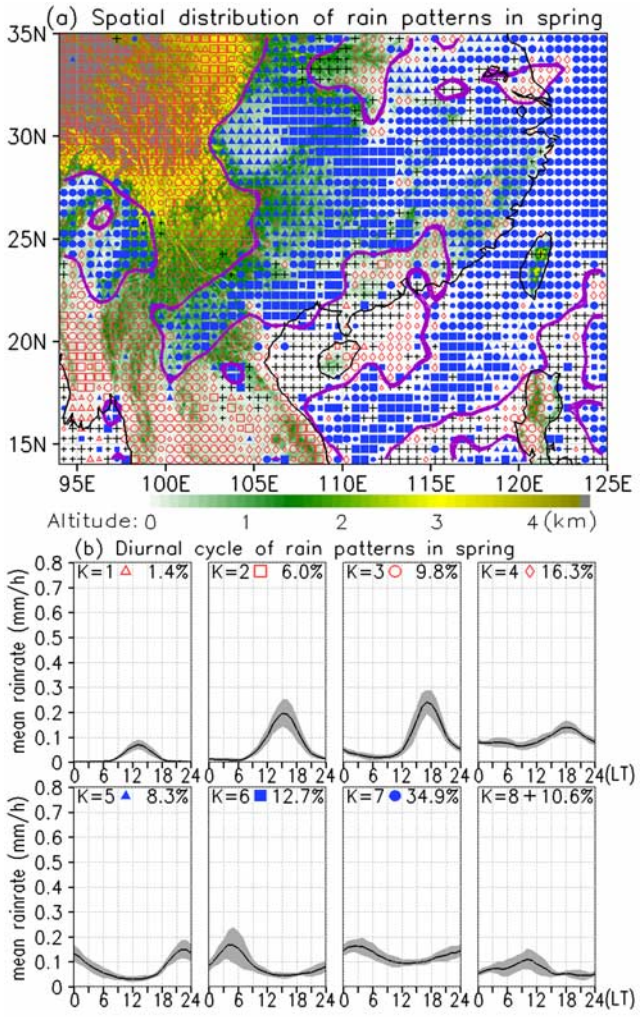

Figure 3. (a) Spatial distribution of rain patterns in spring and (b) their corresponding diurnal cycles of the rain rate along with the standard deviation (shaded). In Figure 3a, the shaded background shows the topography; bold solid contours divide daytime/nighttime rain patterns. The marks of rain patterns K in Figure 3a are labeled at Figure 3b, followed by their contribution percentage to total rainfall over the whole region. Clusters shown at top and bottom of Figure 3b are the daytime and nighttime rain patterns.

north of SEC, however, rainfall of morning hours remains comparable to that of afternoon hours.

4. Seasonal Transition of Diurnal Variability

4.1. Major Patterns of Diurnal Cycles During Spring

[16] To give a detailed map of spatial distribution of the rainfall diurnal cycles, TRMM-TMI rainfall data are analyzed by cluster analysis, as described in section 2.2. Figure 3 shows the characteristic afternoon to early evening rainfall (k = 1–3 in Figure 3) of the Tibetan and Yun-gui plateaus during spring. Rainfall over the high elevation increases after sunrise and reaches a maximum at 1300 LT (k = 1). Such rainfall is relatively weak. The convective ratio undergoes a dramatic oscillation on a diurnal scale (not shown). It increases rapidly during sunrise, reaches its maximum shortly after the noon hour and declines sharply during sunset. Using GMS infrared data, *Fujinami and Yasunari* [2001] also observed active cloud activities that occurred on a diurnal scale, related to dry convection over the Tibetan Plateau during March–April. Along the adjacent slopes, the rainfall is relatively apparent than that over the high elevation, with rainfall peaking at 1600–1800 LT (k = 2,3). The high convective property persists during afternoon and declines gradually through the night (not shown). It corresponds well to the medium-scale convective systems developing along the slopes [*Hirose and Nakamura*, 2005].

[17] At the foot of the Tibetan and Yun-gui plateaus, the rain pattern is identifiable as weak nocturnal rainfall (k = 5). It is interesting that this nocturnal pattern is confined to the Brahmaputra valley and northern Myanmar, but it has a well-defined structure extending to the east flank of those plateaus. Subsequently, it transforms into near-dawn rain patterns over the SEC area (k = 6,7). The frequent activities of stratus clouds were observed to the east leeward of plateaus in spring [*Yu et al.*, 2004]. Nocturnal cooling of clouds might partly contribute to the nocturnal rainfall. It is not clear whether this can explain the nocturnal rain patterns. Furthermore, the eastward phase shift between these rain patterns is apparent at 24–30°N, possibly linked to the migrating cloud streaks [*Wang et al.*, 2004] or long-duration rainfall events [*Yu et al.*, 2007b]. Nevertheless, their underlying processes remain as an open question.

4.2. Major Patterns of Diurnal Cycles During Presummer

[18] During presummer (May–June), the most striking feature is a remarkable enhancement of diurnal cycles (Figure 4). The mean rain rates are more than twice those of spring, as are the amplitudes of diurnal cycles. Over the Tibetan Plateau, three analogous patterns peaking from the afternoon to early evening are found from the high elevation to slopes (k = 1–3 in Figure 4). Results also highlight that the diurnal oscillations of rain rates have large amplitude, with regularly occurring sharp peaks in the afternoon. The convective fraction increases remarkably after sunrise and reaches its maximum at 1300–1500 LT (not shown), when the mean rain rate is increasing rapidly. Consequently, the rainfall is produced by the strong convective systems at 1600–2000 LT. These patterns are in accord with those found in earlier studies, which showed the highest frequency of convective activities in eastern part of the Tibetan Plateau at 1800 LT [*Wang et al.*, 2004; *Hirose and Nakamura*, 2005].

[19] As portrayed in Figure 4, the late night rainfall is found to occur on the east flank of plateaus (k = 5). It gradually evolves to be the morning peak rainfall (k = 6) over western SEC (105–112°E), implying an eastward shift in the phase of diurnal cycles. The maximum rainfall appears at 0500–0900 LT with a rain rate of 0.35 mm/h, the minimum one (0.15 mm/h) being at 1800–2100 LT. Consequently, the large amplitude of diurnal oscillation is exhibited by this rain pattern. East of 112°E, this typical pattern of morning peak rainfall is also observed, especially in valleys and plains. Over the mountain ranges to the east of the Sichuan Basin and those to the north of southern China, morning rainfall has a comparable magnitude to that of afternoon rainfall (k = 7). To the lees of Daba (30–35°N, 110°E) and Dabie-Luoxiao (25–

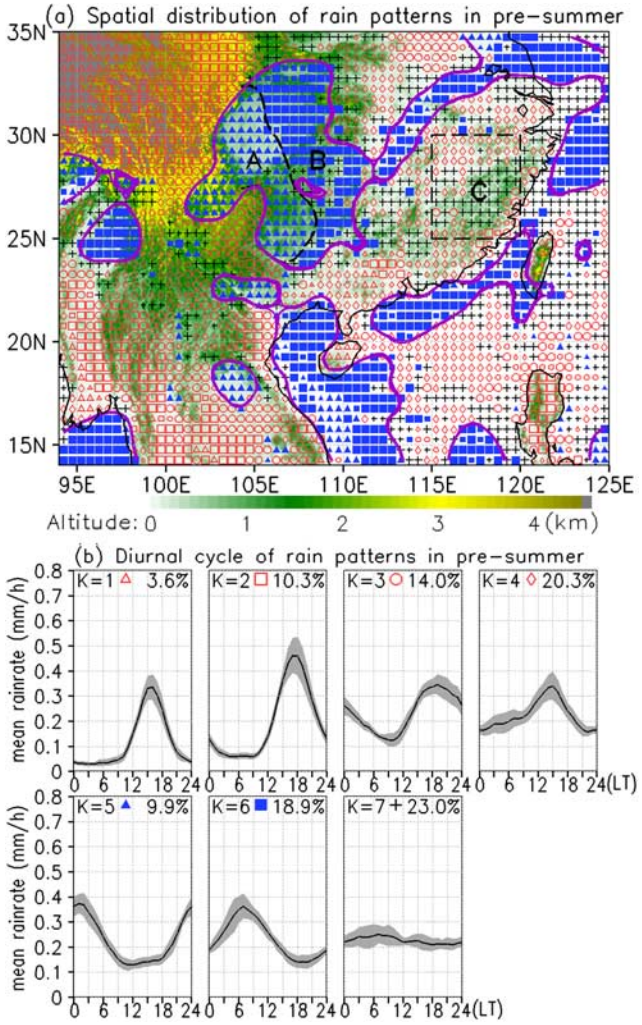

Figure 4. Same as in Figure 3, but for presummer. Regions A, B, and C marked on Figure 4a stand for the east flank of plateaus, western, and eastern SEC, respectively.

30°N, 115°E) mountain ranges, the rain pattern is characterized as an early afternoon peak and a mild increase in the early morning ($k = 4$). Another notable feature is the morning peak rainfall ($k = 6$), which becomes dominant offshore along SEC and the Indochina Peninsula.

[20] A cursory view of Figure 4 reveals the regional-scale differences of rain patterns between the plateaus and basins, between the mountains and valleys, and between the coastal lands and offshore. These results are supportive of previous knowledge related to the regional features of diurnal variation. Using twice daily sounding and surface data, *Johnson et al.* [1993] examined the effects of topography and land-sea contrasts on the diurnal cycles of rainfall. Morning rainfall at lower elevations and evening convection over mountain ranges might result from the diurnally varying local circulation. *Wai et al.* [1996] described the morning maximum of rainfall in the coastal region of Hong Kong, linking it to the interaction of monsoon flow with the secondary circulation. In addition, Figure 4a shows the evident regional contrasts between the east flank of plateaus, the western and eastern SEC. In section 5, we will examine these regional contrasts in detail.

[21] On the other hand, the widespread signature of morning rainfall is highlighted in Figure 4 by major rain patterns over the SEC area (k = 5,6 and part of k = 4,7). These rain patterns clearly show the strong morning rainfall dominating the western SEC and still having apparent signature over the eastern SEC. They begin to be prevalent from presummer when the monsoon flow becomes active. The strong morning rainfall of both the large and regional scales is distinct from the weak nocturnal rainfall in spring, and can be viewed as a unique climatology of presummer over SEC. For this region, it is first shown using the fine-scale data and new methodology. Elucidation of the underlying physics is another goal of this work and will be presented by the continued part.

4.3. Major Patterns of Diurnal Cycles During Midsummer

[22] In midsummer, afternoon to early evening rainfall is observed over plateaus, mountain ranges, and coastal inland areas (k = 1–4 in Figure 5). In contrast, late night to morning rainfall mainly occurs over basins, valleys, plains, and seas (k = 5–7). The spatial distributions of rain patterns are aligned at regular intervals from northwest to southeast regions: from the Tibetan Plateau, Sichuan Basin, mountain

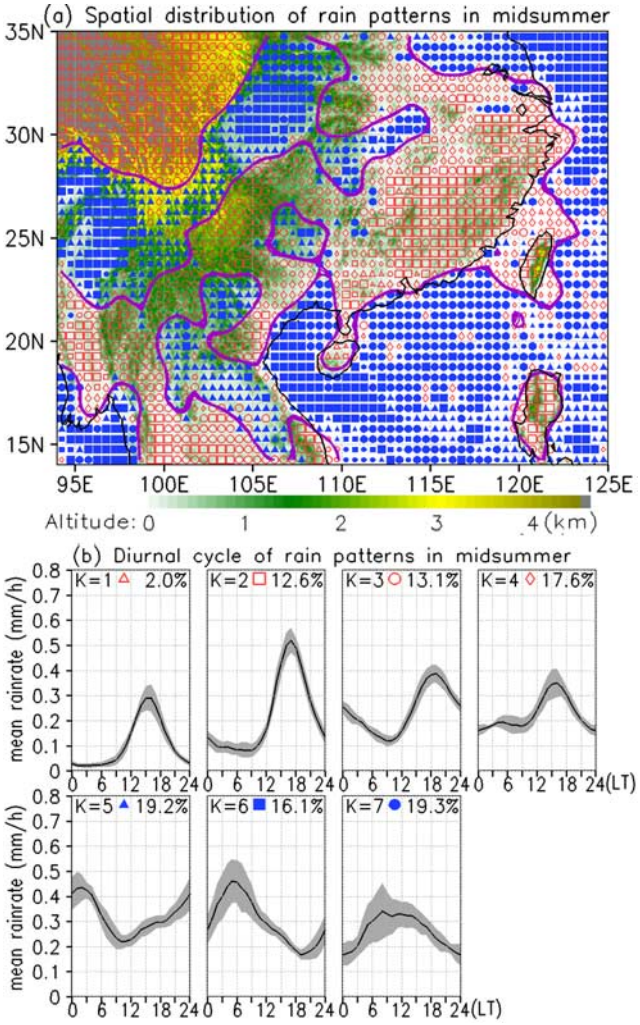

Figure 5. Same as in Figure 3, but for midsummer.

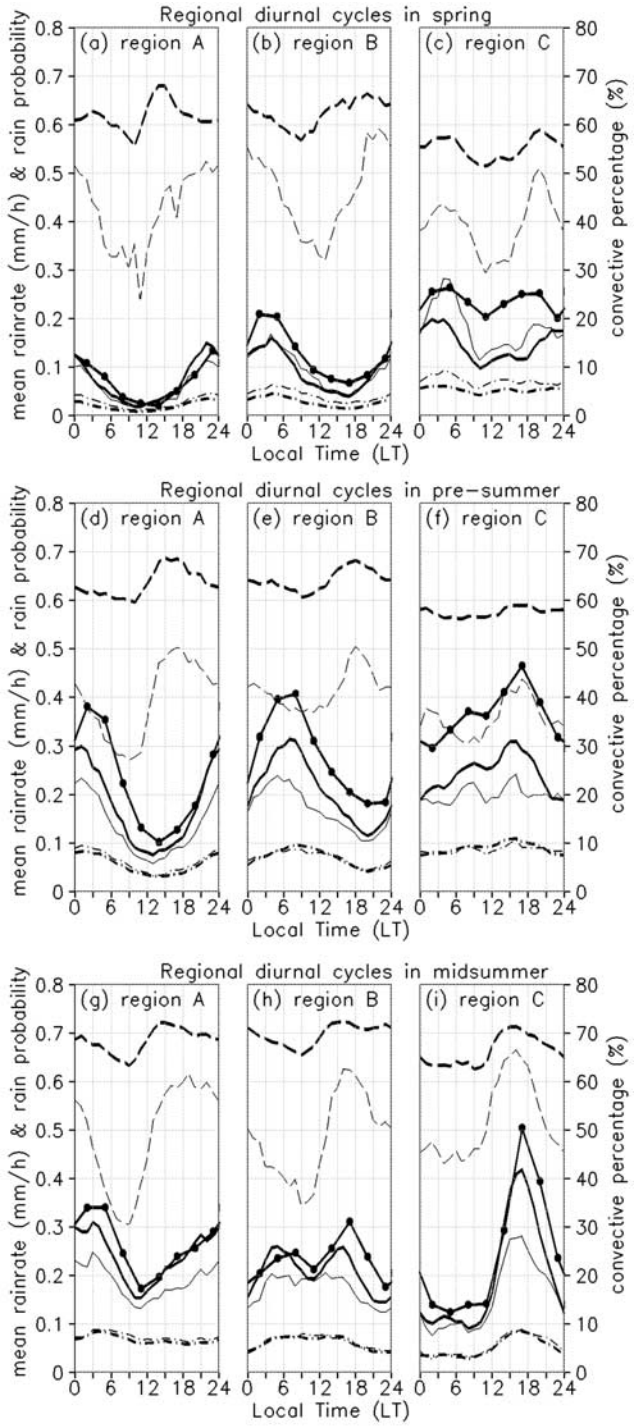

Figure 6. Diurnal cycles of the mean rain rate (solid lines, in units of mm/h), convective percentage (dashed lines, in units of %), and rain probability (dotted-dashed lines, fraction). Regions A, B and C during (a–c) spring, (d–f) presummer, and (g–i) midsummer. Thin lines are derived by TRMM-PR, bold lines are derived by TRMM-TMI, and bold lines with dots are derived by TRMM-3B42.

ranges, and interior plains to the coastal mountains. The pattern of afternoon peak rainfall becomes a notable feature over southern China (k = 2).

[23] In general, Figure 5 vividly shows that the rain patterns in midsummer are closely dependent on topography, which confirms the pioneering work of *Ohsawa et al.* [2001] on the diurnal variation of convective activities during the boreal summer (their Figure 3a). They found that the areas with the late night to early morning maximum in convective activity were clearly separated from those with the afternoon to early evening maximum. On a diurnal scale, this result is also in agreement with the topographical role in anchoring the monsoon precipitation [*Xie et al.*, 2006]. Using cluster analysis of new data in this study, a classification map of rain patterns can be produced with greater clarity than ever before.

[24] Regional features of rain patterns are more pronounced in midsummer than in presummer (cf. Figures 4a and 5a). Meanwhile, the eastward shift in the phases of diurnal cycles between rain patterns over SEC becomes indistinct in midsummer, as found also in earlier studies [*Asai et al.*, 1998; *Wang et al.*, 2004]. Moreover, the morning rainfall once dominating the SEC area during presummer decays in midsummer and leaves only a signature to the north of SEC. Such north shift of morning signature is probably related to the northward march of the summer rainband as shown in Figure 2c. The amplitudes of diurnal oscillations in midsummer are almost coincident with those in presummer, but they are much larger than those in spring. Similarly, an abrupt change of cloud features over southern China takes place during presummer [*Hirasawa et al.*, 1995].

5. Regional Contrasts in Diurnal Variation of Precipitation

[25] A recent study of *Li et al.* [2008] on rain gauge data found that the diurnal cycles over southeastern China might differ in region and duration. Section 4 further shows the spatial difference of rain patterns in a fine scale. On the basis of such fine-scale contrasts, summer transition of diurnal cycles over SEC can be examined in detail. Using the rain estimates by TRMM-TMI, TRMM-PR, and TRMM-3B42, this section compares the diurnal cycles of mean rain rates, convective ratio and rain probability over three key regions of SEC. These regions, between which the striking contrasts of rain patterns exist in presummer, are marked by A, B, and C on Figure 4a. They represent the east flank of plateaus, western and eastern SEC, respectively.

[26] Figure 6 shows that rainfall diurnal cycles by TRMM-TMI generally resemble those by TRMM-PR in terms of diurnal phase or those by TRMM-3B42 in terms of diurnal amplitude. Between them there are discrepancies due to different measurements, resolutions, and retrieval algorithms [*Kummerow et al.*, 2001; *Iguchi et al.*, 2000]. For instance, TRMM-3B42 has the largest but reliable daily mean of rainfall, as it is scaled by the rain gauge monthly observations. As compare to TRMM-PR, TRMM-TMI estimates the higher convective ratio but smaller amplitude of diurnal cycle. Combining these TRMM products is helpful for detailing the contrasts between regions and seasons.

[27] During spring, the daily mean of rainfall amount increases gradually from region A to B and C, as shown in Figures 6a–6c. It is consistent with the spatial distribution of rainfall budget in spring (Figure 2a). Diurnal cycle of

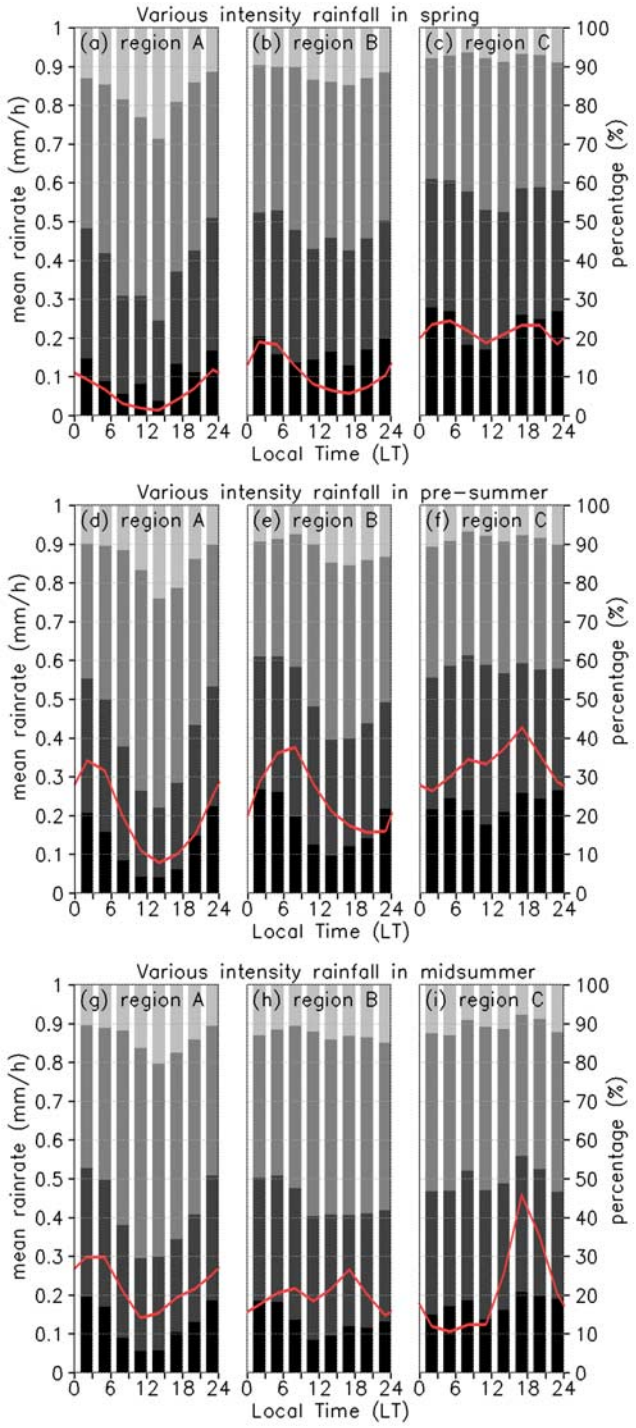

Figure 7. Same as in Figure 6, but for the contribution percentage of various rain rates in 3 hourly TRMM-3B42. From light to dark, the gray bars stand for rain rates of 0–1, 1–4, 4–10, and >10 mm/h, respectively. The bold solid lines show the mean rain rate (mm/h).

rainfall over region A (B) reaches its peak at 2100–2400 LT (0200–0500 LT), when about one half of rainfall amount is categorized as convective by TRMM-PR. Convective percentage has a minimum value of 30% during noon hours. Over region C, in addition to early morning rainfall, afternoon to evening rainfall is observed as a secondary peak (Figure 6c). This peak is comparable to the early morning one in TRMM-3B42; but it is much weaker in other two estimates. In an overview, the weak rainfall peaking at late night or early morning is prevalent over SEC during spring.

[28] To clarify the rain events resulting to regional contrasts, the percentages of various rain rates to rainfall diurnal cycles are examined in Figure 7. Slight, moderate, heavy and extremely heavy rain events are categorized by mean hourly rain rates of 0–1, 1–4, 4–10 and >10 mm/h in 3 hourly TRMM-3B42, respectively. Criterion selection may change daily mean value; the percentage diurnal cycles are quite insensitive to it. A percentage in phase to rainfall indicates extra contribution from that rain rate. Although spring rainfall is weak over regions A and B, its diurnal cycle is largely contributed by moderate or stronger rain rates peaking at midnight or early morning (Figures 7a and 7b). Over region C, intense rain rates (>4 mm/h) contribute more than one half of rainfall amount (Figure 7c). They are also in phase to rainfall diurnal cycle peaking at early morning and afternoon.

[29] Figures 6d–6f show that over three key regions the daily mean rainfall in presummer is double of that in spring. It corresponds well to the seasonal increase of rainfall budget. The large increases in TRMM-TMI estimate are 0.18 mm/h at 0000–0500 LT for region A and at 0600–1100 LT for region B (cf. Figures 6a, 6b, 6d, and 6e). The enhanced rainfall is accompanied by an increase of rain probability, implying an important role of rain frequency in resulting to the rainfall diurnal variation over eastern China [*Zhou et al.*, 2008]. What's striking is the remarkable amplification of diurnal amplitudes over regions A and B. The diurnal amplitudes are 0.22 and 0.2 mm/h, respectively, both compared to ~0.11 mm/h in spring. Diurnal cycle over region A (B) reaches its peak at 0100–0300 LT (0600–0800 LT), with a delay of 3 h from that in spring. Figures 7d and 7e show that the percentages of intense rain rates undergo large diurnal variation peaking at late night and early morning. Note that, moderate (slight) rain rate has its largest contribution through morning and afternoon (at afternoon). Therefore, the intense rain rates, along with the increasing rain frequency, may account for the large amplification of diurnal cycles over regions A and B.

[30] Large increase of rainfall amount, ranging from 0.15 to 0.2 mm/h in both TRMM-TMI and TRMM-3B42, is also observed through the later morning and afternoon over region C (cf. Figures 6c and 6f). It results to a major peak at 1500–1700 LT and a secondary peak at 0800–0900 LT. Although the convective fraction by TRMM-PR has an afternoon maximum, convective property of afternoon rainfall over region C is even lower than that in spring. It indicates other processes rather than daytime convection as major causes for the large increase of rainfall through the later morning and afternoon.

[31] During midsummer, late night to early morning rainfall is still found over region A (Figure 6g). It also has considerable contribution by the diurnally varying intense rain rates (Figure 7g). Diurnal amplitude of rainfall is slightly smaller than that in presummer. In contrast, over region B early morning rainfall related to intense rain rates tends to decline in midsummer (Figures 6h and 7h).

Meanwhile, afternoon maximum of rainfall becomes obvious over there. These two peaks have a comparable magnitude in TRMM-TMI, while the afternoon one is stronger in TRMM-3B42. Similar remarkable change is also observed over region C, where the midsummer rainfall is characterized by a sharp peak at 1500–1700 LT (Figures 6i and 7i). Over these three regions, the convective fractions undergo large increase both in daily mean and diurnal amplitude. There are about 60% of the afternoon rainfall categorized as convective, while only 40–50% in presummer. The prevalent afternoon convection over region C is primarily induced by the solar heating during daytime [*Kato et al.*, 1995].

6. Summary and Concluding Remarks

[32] Southeastern China (SEC), because of its unique location, is an ideal domain for studying the rainfall diurnal variability during the seasonal march of East Asian rainband. The motives of this study were to document a detailed picture for diurnal variation over this key region. Using the fine-scale satellite rainfall, the representative spatial patterns and diurnal cycles were identified in both the large and regional scales. The major findings are summarized as follows:

[33] 1. In spring and presummer, rainfall during 0000–1200 LT contributes considerably to the rainfall budget over SEC, where the seasonal rainband is located. Over the western SEC, in excess of 20% more rainfall amount falls during 0000–1200 LT than during 1200–2400 LT. Even over the eastern SEC, rainfall amount during 0000–1200 LT still has a comparable magnitude to that during 1200–2400 LT. In midsummer, however, morning signature of rainfall decays and shifts to the north of SEC, in accord with the northward march of the seasonal rainband.

[34] 2. Rainfall diurnal cycles and their spatial distributions display the remarkable seasonality over SEC. The weak nocturnal rainfall is prevalent during spring. In contrast, major rain patterns in presummer have the stronger mean rain rates and larger amplitudes of diurnal cycles. Among them, the late night rainfall occurs on the east flank of plateaus; to its east the morning peak rainfall dominates the western SEC. Even over the eastern SEC, the morning signature of rainfall remains visible, although afternoon rainfall is readily observed there. During midsummer, however, the terrain-dependent rain patterns become dominant the SEC area. Afternoon to early evening rainfall appears over the plateaus, mountains, and coastal inland regions especially southern China; late night to morning rainfall appears over the basins, valleys, plains, and seas.

[35] 3. Regional analysis shows that the diurnal amplitude increases from ~0.11 mm/h in spring to 0.2 mm/h in presummer over western SEC. The strong morning rainfall may result from the diurnally varying intense rain rates and the increasing rain frequency. Contribution percentages of the intense rain rates undergo large diurnal variation: they reach the maximums at the early morning, slightly leading to the large seasonal increase (0.18 mm/h at 0600–1100 LT) of rainfall diurnal cycle over western SEC. The enhanced rainfall is also accompanied by a large increase of rain probability in the morning.

[36] 4. Presummer rainfall over eastern SEC is distinct having a large seasonal increase (0.15–0.2 mm/h) through later morning and afternoon. As a result, rainfall diurnal cycle has a major peak at 1500–1700 LT and a secondary peak at 0800–0900 LT. The convective property of rainfall is relative low in presummer, although it has an afternoon maximum. The large contribution of intense rain rates is also observed but with weaker diurnal variation.

[37] Spatial distributions of diurnal cycles and their seasonality are helpful for revealing the underlying physics. It is interesting, the seasonal increase of rainfall from spring to presummer takes place through morning over western SEC and till afternoon over the east. It seems to be more complex than attributed to nocturnal cooling of clouds or to afternoon convection induced by surface heating. Besides, the low and middle stratiform cloudiness decreases from spring to presummer [*Li et al.*, 2004]. Recent analysis shows that the early morning peak on the east flank of plateaus mainly results from long-duration rain events [*Yu et al.*, 2007b]. This study also reveals that the morning rainfall tends to occur along the East Asian rainband and closely relates to intense rain rates. As indicated above, the organized precipitation systems having prolonged duration along the quasi-stationary front during presummer need to be concerned, when addressing the mechanism responsible for these distinct diurnal cycles. It is speculated, diurnally varying monsoon flow may regulate favorable conditions for the development of precipitation systems and hence rainfall diurnal cycles. The continued part of this work will present an investigation on this possible mechanism.

[38] In addition to the widespread strong morning rainfall, regional features are evidently shown in presummer. To clarify the regional-scale diurnal cycles, *Johnson et al.* [1993] emphasized the effects of topography on the diurnally varying local circulation. It is also proposed that the interaction of monsoon flow with the secondary circulation may account for the morning maximum of rainfall in coastal region [*Wai et al.*, 1996]. The present study has shown a remarkable amplification of morning rainfall over western SEC during presummer. Such amplification is probably related to the sufficient water vapor by monsoon flow. However, it is not clear whether the diurnal-scale coupling between local circulation and monsoon flow explain the enhanced morning rainfall over western SEC. The low-level circulation on a regional scale must be clarified to explain such regional features revealed in the present study. This issue might be addressed in the future using high-resolution data derived by numerical simulations or field experiments.

[39] **Acknowledgments.** The authors are grateful to the reviewers and the chief editor, Steve Ghan, for very constructive suggestions. They thank Jun Matsumoto and Takehiko Satomura for their valuable comments during MAHASRI workshop. They also appreciate the help and support from Tetsuzo Yasunari of the Hydrospheric Atmospheric Research Center (HyARC), Nagoya University. This work has been supported by the joint research funding from HyARC.

References

Asai, T., S. Ke, and Y. Kodama (1998), Diurnal variability of cloudiness over East Asia and the western Pacific Ocean as revealed by GMS during the warm season, *J. Meteorol. Soc. Jpn.*, *76*(5), 675–684.

Carbone, R. E., J. D. Tuttle, D. A. Ahijevych, and S. B. Trier (2002), Inferences of predictability associated with warm season precipitation episodes, *J. Atmos. Sci.*, *59*(13), 2033–2056, doi:10.1175/1520-0469(2002)059<2033:IOPAWW>2.0.CO;2.

Ding, Y. (1992), Summer monsoon rainfalls in China, *J. Meteorol. Soc. Jpn.*, *70*(1B), 373–396.

Fujibe, F. (1999), Diurnal variation in the frequency of heavy precipitation in Japan, *J. Meteorol. Soc. Jpn.*, *77*(6), 1137–1149.

Fujinami, H., and T. Yasunari (2001), The seasonal and intraseasonal variability of diurnal cloud activity over the Tibetan Plateau, *J. Meteorol. Soc. Jpn.*, *79*(6), 1207–1227, doi:10.2151/jmsj.79.1207.

Hirasawa, N., K. Kato, and T. Takeda (1995), Abrupt change in the characteristic of the cloud zone in subtropical East Asia around the middle of May, *J. Meteorol. Soc. Jpn.*, *73*(2), 221–239.

Hirose, M., and K. Nakamura (2005), Spatial and diurnal variation of precipitation systems over Asia observed by the TRMM Precipitation Radar, *J. Geophys. Res.*, *110*, D05106, doi:10.1029/2004JD004815.

Iguchi, T., T. Kozu, R. Meneghini, J. Awaka, and K. Okamoto (2000), Rain-profiling algorithm for the TRMM precipitation radar, *J. Appl. Meteorol.*, *39*(12), 2038–2052, doi:10.1175/1520-0450(2001)040<2038:RPAFTT>2.0.CO;2.

Johnson, R. H., Z. Wang, and J. F. Bresch (1993), Heat and moisture budgets over China during the early summer monsoon, *J. Meteorol. Soc. Jpn.*, *71*(1), 137–152.

Kato, K., J. Matsumoto, and H. Iwasaki (1995), Diurnal variation of Cb-clusters over China and its relation to large-scale conditions in the summer of 1979, *J. Meteorol. Soc. Jpn.*, *73*(6), 1219–1234.

Kummerow, C., et al. (2001), The evolution of the Goddard Profiling Algorithm (GPROF) for rainfall estimation from passive microwave sensors, *J. Appl. Meteorol.*, *40*(11), 1801–1820, doi:10.1175/1520-0450(2001)040<1801:TEOTGP>2.0.CO;2.

Li, J., R. Yu, and T. Zhou (2008), Seasonal variation of the diurnal cycle of rainfall in southern contiguous China, *J. Clim.*, *21*(22), 6036–6043, doi:10.1175/2008JCLI2188.1.

Li, Y., R. Yu, Y. Xu, and X. Zhang (2004), Spatial distribution and seasonal variation of cloud over China based on ISCCP data and surface observations, *J. Meteorol. Soc. Jpn.*, *82*(2), 761–773, doi:10.2151/jmsj.2004.761.

Luo, H., and M. Yanai (1984), The large-scale circulation and heat-sources over the Tibetan Plateau and surrounding areas during the early summer of 1979. Part 1. Heat and moisture budgets, *Mon. Weather Rev.*, *112*(5), 966–989, doi:10.1175/1520-0493(1984)112<0966:TLSCAH>2.0.CO;2.

Nesbitt, S. W., and E. J. Zipser (2003), The diurnal cycle of rainfall and convective intensity according to three years of TRMM measurements, *J. Clim.*, *16*, 1456–1475.

Nesbitt, S. W., R. Cifelli, and S. A. Rutledge (2006), Storm morphology and rainfall characteristics of TRMM precipitation features, *Mon. Weather Rev.*, *134*(10), 2702–2721, doi:10.1175/MWR3200.1.

Nitta, T., and S. Sekine (1994), Diurnal-variation of convective activity over the tropical western Pacific, *J. Meteorol. Soc. Jpn.*, *72*(5), 627–641.

Ohsawa, T., H. Ueda, T. Hayashi, A. Watanabe, and J. Matsumoto (2001), Diurnal variations of convective activity and rainfall in tropical Asia, *J. Meteorol. Soc. Jpn.*, *79*(1B), 333–352, doi:10.2151/jmsj.79.333.

Takeda, T., and H. Iwasaki (1987), Some characteristics of meso-scale cloud clusters observed in East Asia between March and October 1980, *J. Meteorol. Soc. Jpn.*, *65*(3), 507–513.

Tao, S., and L. Chen (1987), A review of recent research on the East Asian summer monsoon in China, in *Monsoon Meteorology*, edited by C.-P. Chang and T. N. Krishnamurti, pp. 60–92, Oxford Univ. Press, New York.

Wai, M. M. K., P. T. Welsh, and W. M. Ma (1996), Interaction of secondary circulations with the summer monsoon and diurnal rainfall over Hong Kong, *Boundary Layer Meteorol.*, *81*(2), 123–146, doi:10.1007/BF00119062.

Wallace, J. M. (1975), Diurnal variations in precipitation and thunderstorm frequency over the conterminous United States, *Mon. Weather Rev.*, *103*(5), 406–419, doi:10.1175/1520-0493(1975)103<0406:DVIPAT>2.0.CO;2.

Wang, C. C., G. T. J. Chen, and R. E. Carbone (2004), A climatology of warm-season cloud patterns over East Asia based on GMS infrared brightness temperature observations, *Mon. Weather Rev.*, *132*(7), 1606–1629, doi:10.1175/1520-0493(2004)132<1606:ACOWCP>2.0.CO;2.

Xie, S. P., H. Xu, N. H. Saji, and Y. Wang (2006), Role of narrow mountains in large-scale organization of Asian monsoon convection, *J. Clim.*, *19*(14), 3420–3429, doi:10.1175/JCLI3777.1.

Yang, S., and E. A. Smith (2006), Mechanisms for diurnal variability of global tropical rainfall observed from TRMM, *J. Clim.*, *19*(20), 5190–5226, doi:10.1175/JCLI3883.1.

Yu, R., B. Wang, and T. Zhou (2004), Climate effects of the deep continental stratus clouds generated by the Tibetan Plateau, *J. Clim.*, *17*(13), 2702–2713, doi:10.1175/1520-0442(2004)017<2702:CEOTDC>2.0.CO;2.

Yu, R., T. Zhou, A. Xiong, Y. Zhu, and J. Li (2007a), Diurnal variations of summer precipitation over contiguous China, *Geophys. Res. Lett.*, *34*, L01704, doi:10.1029/2006GL028129.

Yu, R., Y. Xu, T. Zhou, and J. Li (2007b), Relation between rainfall duration and diurnal variation in the warm season precipitation over central eastern China, *Geophys. Res. Lett.*, *34*, L13703, doi:10.1029/2007GL030315.

Zhou, T., R. Yu, H. Chen, A. Dai, and Y. Pan (2008), Summer precipitation frequency, intensity, and diurnal cycle over China: A comparison of satellite data with rain gauge observations, *J. Clim.*, *21*(16), 3997–4010, doi:10.1175/2008JCLI2028.1.

G. Chen, T. Iwasaki, and W. Sha, Department of Geophysics, Graduate School of Science, Tohoku University, 6-3 Aoba Aramaki, 980-8578 Sendai, Japan. (chen@wind.geophys.tohoku.ac.jp)